

Static and dynamic structure and the atomic dynamics of liquid Ge from first-principles molecular-dynamics simulations

S. Munejiri* and T. Masaki†

Japan Aerospace Exploration Agency (JAXA), 2-1-1 Sengen, Tsukuba, 305-8505, Japan

T. Itami‡

Division of Chemistry, Graduate School of Science, Hokkaido University, N10W8, Kita-ku, Sapporo, 060-0810, Japan

F. Shimojo

Graduate School of Science and Technology, Kumamoto University, Kumamoto, 860-8555, Japan

K. Hoshino

Graduate School of Integrated Arts and Sciences, Hiroshima University, Higashi-Hiroshima, 739-8521, Japan

(Received 19 July 2007; revised manuscript received 1 November 2007; published 18 January 2008)

The first-principles molecular-dynamics simulation was performed for liquid Ge at 1253 K by using two kinds of simulation cells: The cubic cell of 64 atoms and the rectangular parallelepiped one of 128 atoms. The rectangular parallelepiped cell of 128 atoms was adopted to obtain the dynamic structure factor of liquid Ge in the small wave number region. The long simulation time was adopted, i.e., 66 ps for the cubic cell and 75 ps for the rectangular parallelepiped one. The present first-principles molecular-dynamics simulation reproduces well the experimental static structure factor and radial distribution function. A broad peak around 100° in the obtained bond angle distribution function implies the existence of the tetrahedral atomic unit in liquid Ge. The self-diffusion coefficient for the rectangular parallelepiped cell is 20% larger than that of the cubic one. The obtained dynamic structure factor agrees well with the experimental one obtained by the inelastic x-ray scattering experiment [Hosokawa *et al.*, Phys. Rev. B **63**, 134205 (2001)], which shows the “de Gennes narrowing” of the main peak and the existence of the side peaks. These side peaks represent a longitudinal vibrational motion, which was also supported by the subsidiary peak around 30 ps^{-1} in the spectral density of the velocity autocorrelation function. The gradient of the dispersion relation in the present simulation agrees well with the experimental sound velocity. This “no positive dispersion” accords well with the inelastic x-ray scattering experiment of Hosokawa *et al.* The reason for this “no positive dispersion” for liquid Ge is discussed in particular concern with its low kinematic viscosity. Though the velocity autocorrelation function itself does not show a cage effect, a microscopic cage effect can be found by the detailed analysis for the trace and environment of the single atomic motion. The atomic movement as a group of 3–5 atoms seems to be present in liquid Ge in addition to individual atomic motions. The covalent bond seems to be also present at least instantaneously in liquid Ge.

DOI: [10.1103/PhysRevB.77.014206](https://doi.org/10.1103/PhysRevB.77.014206)

PACS number(s): 61.20.Ne, 61.20.Ja, 61.20.Lc, 66.10.–x

I. INTRODUCTION

The structure of liquid Ge is complicated compared with that of simple liquid metals, such as liquid alkali metals. Unlike simple liquid metals, the structure factor, $S(Q)$, of liquid Ge has a shoulder in the high Q (Q : wave number) side of the main peak.^{1–5} Similar shoulders can be seen for some group 13, 14, and 15 elements in the liquid state.¹ Particularly a systematic increasing tendency with the decrease of the atomic mass^{6–9} can be seen for such a shoulder in the $S(Q)$'s of the group 14 elements in the liquid state. Harada *et al.*⁹ showed the similar systematic variation of the shoulder among group 14 elements in the liquid state including the $S(Q)$ of liquid carbon, which was obtained by the first-principles molecular-dynamics (FPMD) simulation. The origin of this shoulder has been discussed from various points of view,⁶ such as a double hard sphere model,^{10,11} the distorted β -Sn structure¹² based on the reverse Monte Carlo analysis of the experimental $S(Q)$, the existence of the ledge in the interionic pair potential,^{13–16} the ledge (or wiggle) in

the interionic pair potential due to the interplay between the effective core radius and the wavelength of the Friedel oscillation,^{7,17} the Peierls distortion or Kohn anomaly,¹⁸ and the polarization effect of ion cores^{19,20} or the existence of the cluster units (or many body potential) even in liquid metals.²¹ The role of this ledge in the interionic pair potential^{7,8} was also applied to explain the systematic variation of liquid structures among the group 14 elements (Si, Ge, Sn, and Pb). Even the systematic trend of the crystal structures in the periodic table has been explained from this interplay of two characteristic lengths in the interionic pair potentials.²²

Recently, Itami *et al.*⁶ showed by the neutron scattering (NS) experiment the existence of the shoulder in the first peak of $S(Q)$ for liquid Sn even at 1873 K, which is far higher temperature than the melting temperature, T_m and by their FPMD simulation an evidence of at least the fragment of the tetrahedral atomic group in liquid Sn. In addition, the $S(Q)$'s of group 14 elements in the liquid state are classified into two categories,²³ densely packed liquids (Pb, Sn) and

loosely packed ones (Ge, Si). The latter group in the solid state is a semiconductor, which has a diamond structure connected by a covalent bond. The former group in the solid state has a metallic character which is derived from rather a closely packed structure. Still now, it is open to question whether the atomic group connected by the covalent bond is still present or not in liquid metals whose $S(Q)$'s show the shoulder in the high Q side of their first peak. Therefore, it is important to clarify experimentally and theoretically the microscopic feature of the structure of liquid Ge, for which the $S(Q)$ has a far more distinct shoulder than that of liquid Sn. The experimental condition for liquid Ge is not so severe compared with that of liquid Si due to its lower T_m and less corrosive properties. It is very important to study the static and dynamic structures and physical properties of liquid Ge in detail as a representative of liquid metals with such shoulders.

From the interest in the effect of covalent bond on the physical properties of liquids, many physical properties have been studied for liquid semiconductors including liquid Ge and Si.^{24,25} The atomic transport properties are expected to be strongly dependent on the covalent bond in liquids if present. The self-diffusion coefficient, D , has been measured also for liquid Ge on the ground²⁶ and even under microgravity.^{27,28} Recent accurate experimental data of viscosity by Sato *et al.*^{29,30} show that liquid Si and Ge are not so viscous even just above the T_m . Itami *et al.*²³ explained qualitatively based on the hard sphere model that the low viscosity of liquid Si and Ge is derived from their loosely packed structures. The role of packing and covalent bonds on the structure and physical properties of liquid Ge must be analyzed in detail from more fundamental point of view.

The dynamic structure factor, $S(Q, \omega)$ is the most fundamental property for atomic dynamics in condensed matters. Under the situation of no experimental data available for the comparison, a preliminary theoretical calculation¹⁸ of the $S(Q, \omega)$ was performed for liquid Ge based on the viscoelastic theory.³¹⁻³³ At present, the experimental $S(Q, \omega)$ is available for liquid Ge at 1253 K (Ref. 34) and 1773 K (Ref. 35) and even for liquid Si at 1733 K (Ref. 36) from the inelastic x-ray scattering (IXS) experiments by Hosokawa *et al.* The characteristic features of the $S(Q, \omega)$ of liquid metals (or liquids)³⁷ are the existence of the narrowing of the main peak around the Q_P [Q_P : Q corresponding to the first peak of $S(Q)$] ("de Gennes narrowing") and the existence of the side peaks around the main peak in the Q range below the $Q_P/2$. These side peaks are derived from the longitudinal vibrational mode.³¹⁻³³ In the low Q region, a linear relation was found in the dispersion relation, which can be obtained in principle from the peak angular frequency, ω_p , of these side peaks as a function of the Q . These particular features of the $S(Q, \omega)$ were also observed for liquid Ge.^{34,35} However, the gradient of the dispersion relation near $Q=0$ for liquid Ge accords well with the experimental velocity of sound³⁸ ("no positive dispersion"). Hereafter, when the gradient of dispersion curve in low Q region is larger (smaller) than the experimental velocity of sound, v_s , we call its characteristic feature the positive (negative) dispersion (e.g., Ref. 37). In addition, when it accords with the v_s , we call this phenomenon "no positive dispersion."

Until now almost all studies about the $S(Q, \omega)$ of liquids have shown the "positive dispersion," as can be seen for many liquid metals,³⁷ expanded liquid Hg,³⁹ liquid NaCl,⁴⁰ water,⁴¹⁻⁴³ and liquid CCl₄ (Ref. 44) and even for glasses.⁴⁵⁻⁴⁷ Bove *et al.*⁴⁸ showed that the almost same positive dispersion relation can be observed for liquid Ga regardless of experimental tools, IXS technique, or inelastic neutron scattering (INS) one, or molecular-dynamics (MD) simulation. According to Table I in the previous review,³⁷ only two exceptions among 25 liquid metals can be seen, that is, "no positive dispersion" for liquid Ge (Refs. 34 and 35) and "negative dispersion" for liquid Ni.⁴⁹ The "no positive dispersion" for liquid Ge, which was reported by the IXS experiment by Hosokawa *et al.*,^{34,35} is quite curious judging from the fact that the dispersion relation for liquid Si, which seems to be a similar liquid to liquid Ge, shows a considerably large "positive dispersion."³⁶ Scopigno *et al.*³⁷ also, in their excellent review, stressed the necessity of further experimental investigations particularly about the "no positive dispersion" of liquid Ge. However, it is a fact that the "no positive dispersion" for liquid Ge was reproduced by the theoretical calculation of Hoshino^{50,51} based on the viscoelastic theory,³¹⁻³³ though predicted side peaks are a little larger compared with experimental ones.³⁴ Therefore, it is important to study further the $S(Q, \omega)$ of liquid Ge by using a reliable MD simulation.

The classical MD simulations, which are based on the Newton's equation of motion, were reported for liquid Ge by Arnold *et al.*⁵² and Yu *et al.*,⁵³ who were concerned with rather static properties of liquid Ge. In addition, the interionic pair potentials employed by them contain some ambiguity such as the adoption of the nearly free electron model⁵⁴ or the empirical model form and parameters⁵⁵ for many-body potential. For complex liquids including liquid Ge, Ashcroft²¹ stressed the importance of many-body potential with rigorous theoretical basis. The FPMD simulation, which is based on the quantum mechanical density functional theory for the many electrons system,⁵⁶ is useful because of its freedom from the interionic potential.

Up to date, such FPMD simulations for liquid Ge have been reported by Kresse and Hafner,^{56,57} Takeuchi and Garzón,⁵⁸ Kulkarni *et al.*,⁵⁹ Munejiri *et al.*,⁶⁰ Chai *et al.*,⁶¹ and Hugouvieux *et al.*⁶² The first four studies⁵⁶⁻⁵⁹ provided the discussions mainly about various static properties, such as $S(Q)$, radial distribution function, $g(r)$, and bond angle distribution function, $g^{(3)}(\theta, r)$. In addition, these studies discussed some properties related to the atomic dynamics, such as mean square displacement (MSD), velocity autocorrelation function (VAF), $Z(t)$, its spectral density, $\tilde{Z}(\omega)$, and D . These simulations reproduced the shoulder of the experimental $S(Q)$ for liquid Ge. In addition, they have well reproduced the experimental $g(r)$, particularly the flat shape or the small hump between its first peak and second one, which is known as a characteristic feature of the experimental $g(r)$ for liquid Ge.^{1,8} However, the dynamic structure factor, $S(Q, \omega)$, was not evaluated in these studies. Munejiri *et al.*⁶⁰ have already reported the preliminary calculation of the $S(Q, \omega)$ based on the FPMD simulation with a boundary condition of a cubic cell of 64 atoms and a simulation time of 66 ps. Chai *et al.*⁶¹

also presented the $S(Q, \omega)$ of liquid Ge by means of the FPMD simulation with a similar boundary condition and a simulation time of 16 ps. The “de Gennes narrowing” of the $S(Q, \omega)$ was reproduced by these FPMD simulations^{60,61} in the larger Q range (over 5.6 nm^{-1}), which does not cover the low Q one required for the comparison of the calculated dispersion relation with the IXS experiment ($2.0\text{--}28 \text{ nm}^{-1}$) by Hosokawa *et al.*³⁴ Hugouvieux *et al.*⁶² reported the FPMD simulation of 30 ps based on the VASP code for liquid Ge. The dispersion relation was also discussed, though, in addition to larger Q range ($7\text{--}11 \text{ nm}^{-1}$), adopted temperatures were different from the experimental ones of Hosokawa *et al.*^{34,35} Therefore, at present the detailed study of the FPMD simulations is desired for the analysis of the dispersion relation for liquid Ge.

According to the general trend of the ω_p ,^{31–33} with the increase of the Q the ω_p increases linearly near $Q=0$, then it shows a suppression tendency followed by a maximum around the $Q_p/2$ and then a minimum at the Q_p . This suppression tendency of the ω_p may be derived from the “structural effect,” which was clearly shown for liquid Li by the antiphase variation of the ω_p against the $S(Q)$.^{37,63} The “positive dispersion” of liquids has been interpreted based on the generalized hydrodynamics³¹ as the crossover from the hydrodynamic behavior to the viscoelastic one. From this approach, the solidlike response in liquids is responsible for the “positive dispersion.”³¹ Based on this theory, Hosokawa *et al.*^{34,35} concluded that the “positive dispersion” for liquid Ge should be present in the energy range beyond 7.8 meV (Ref. 34) or 16.7 meV.³⁵ Unfortunately the “positive dispersion” in this energy range may be masked by the suppression tendency in the dispersion relation due to the “structural effect” described above. The close relation of the atomic dynamics in liquids to that in solids was reported for liquid K by Cabrillo *et al.*⁶⁴ and Bove *et al.*⁶⁵ by the INS experiment. Balucani and Zoppi³³ showed a possibility that the “positive dispersion” should be more distinct for liquids with a “harsh” interatomic pair potential than those with a “soft” one by considering the role of so called Einstein frequency. With the increase of the Einstein frequency for the “harsh” interionic pair potential, the viscoelasticity is expected to increase.

As the origin of this “positive dispersion” Scopigno *et al.*^{37,63} presented an idea quite different from above view points derived from the solidlike behavior. They considered that there exist two channels⁶³ for the relaxation of the atomic dynamics in liquid Li, one is the slower structural relaxation and the other is the faster relaxation. They concluded that the “positive dispersion” is strongly related to the faster relaxation, which may originate from the general relaxation process peculiar to the vibrational dynamics. This view point may be consistent with the existence of the “positive dispersion” for almost all kinds of liquids and even for glasses as described above. Such a two-exponential decay of the memory function was introduced previously also by Levesque *et al.*⁶⁶ Particularly concerned with the “positive dispersion” of glasses, Song-Ho Chong⁶⁷ recently presented the theory of dispersion relation for glasses with a Lenard-Jones potential based on the mode-coupling analysis.⁶⁸ In this analysis such two processes, the structural relaxation and

the vibrational one called as the anomalous oscillation peak (AOP), were taken into account. The “positive dispersion” for the liquid state was reproduced successfully. Even the possibility of the “negative dispersion” was pointed out for the deep-in-glass state. However, the application of this approach seems to be not appropriate for liquid Ge because the mode-coupling (MC) theory, which is the basis of Song-Ho Chong’s theory, is not valid to liquid Ge, as described below. Therefore, the application of the MC theory does not seem to be a unique answer to solve the problem of the “no positive dispersion” for liquid Ge, though it is valid to explain the “positive dispersion” in the wide range of the state from liquid to glass.^{37,67} It is very important to study the dispersion relation of liquid Ge by the reliable FPMD simulation.

The atomic dynamics has been discussed successfully also from the MC theory,^{31–33} mainly for simple liquid metals, like liquid alkali metals near the melting temperature.^{69–73} As shown by Gudowski *et al.*,⁷⁴ this MC analysis is not always valid for liquid Pb because of its positively repulsive interionic pair potential. Hoshino *et al.*⁷⁵ concluded that the MC theory is invalid for liquid Na at 900 K and for liquid Ge and Sn even near the T_m , though it is valid for liquid Na near the T_m . These studies indicate that the MC theory is not valid for liquid metals with a positively repulsive interionic pair potential (liquid Pb and Ge) and a interionic pair potential showing a shallow minimum (liquid Sn near the T_m and liquid Na at 900 K). Under such interionic pair potentials, a required condition for the MC theory may be broken down, that is, a free particlelike motion, corresponding to the short time decay of the binary collision effect, is restrained due to the coupling of atomic motion with neighboring atoms.^{74,75} This breakdown of the MC theory for liquid Na at 900 K (Ref. 75) seems to warn us of the limitation of the MC theory for the explanation of “positive dispersion,” because the “positive dispersion” itself was found experimentally for liquid Na (Refs. 37 and 76) up to the higher temperature of 1173 K. It is a fact that at present the most promising analysis of the atomic dynamics in liquids is the MC theory. Therefore, other theoretical tools must be applied to clarify the atomic dynamics in liquid Ge. In this respect, it is very important to perform a reliable FPMD simulation, which is free from theories described above.

For the acquirement of the reliable $S(Q, \omega)$ from the FPMD simulation, it is important to adopt a long simulation time and to realize a small Q value. Such a small Q value can be obtained by the adoption of the simulation cell with a large size. For this purpose, in the present FPMD study, a rectangular parallelepiped cell was adopted. Following the preliminary report,⁶⁰ the present paper describes fully the results of the FPMD study for liquid Ge at 1253 K, which was performed by using both the cubic cell of 64 particles with a simulation time of 66 ps and the rectangular parallelepiped cell of 128 particles with a longer one of 75 ps. The system size dependence of the D and other physical properties was also investigated. In addition, the $S(Q, \omega)$ and the atomic dynamics were analyzed in detail. In Sec. II, the method of the present FPMD simulation is described particularly in detail for the dynamic structure factors and dynamic properties. In Sec. III obtained results in the present FPMD simulation are described fully for the static and dy-

dynamic properties of liquid Ge, more specifically $S(Q)$, $g(r)$, $g^{(3)}(\theta, r)$, coordination number distribution, MSD, VAF, D , $\tilde{Z}(\omega)$, $S(Q, \omega)$, dispersion relation, and the trace and environment of the single atomic motion.

II. METHOD OF THE FIRST-PRINCIPLES MOLECULAR-DYNAMICS (FPMD) SIMULATIONS

The present first-principles molecular-dynamics (FPMD) simulation was based on the density functional theory in which the generalized gradient approximation⁷⁷ was adopted for the exchange-correlation energy. Employed interaction between the valence electrons and the ions is the norm-conserving pseudopotential,^{56,57} which was evaluated for the electron configuration of $4s^2 4p^2 4d^0$ for Ge atoms. The electronic wave functions at the Γ -point of the Brillouin zone were expanded by a plane wave basis set with a cutoff energy of 11 Ryd. The Kohn-Sham energy functional was minimized by the preconditioned conjugate-gradient method.^{56,57,78,79} The FPMD simulation of constant temperature condition was carried out by using the Nose⁸⁰-Hoover⁸¹ thermostat.

The adopted number density of the system, n , was 46.58 nm^{-3} , which was calculated from the experimental density of liquid Ge at 1253 K.⁸² The FPMD simulation with a periodic boundary condition was carried out by using 64 atoms in a cubic cell (system 1). The sidelength of the FPMD supercell, L , was 1.111 nm. To calculate the dynamic structure factor accurately, we performed a long-time FPMD simulation of 66 ps, which corresponds to 22 000 steps [one step: 125 a.u. (3.02 fs)]. Physical properties were calculated by averaging over atomic configurations of 21 500 steps after the thermodynamic equilibrium was established. In the system 1, the smallest wave number, Q_{\min} , was 5.7 nm^{-1} ($=2\pi/L$). On the other hand, experimental dynamic structure factors were reported for $2.0 \text{ nm}^{-1} < Q < 28.0 \text{ nm}^{-1}$.³⁴ To obtain the dynamic structure factor, $S(Q, \omega)$, in the smaller Q region in the FPMD simulation, a larger system of 128 atoms (system 2) was also adopted in addition to the system 1. The adopted FPMD supercell of the system 2 was not a cubic box but a rectangular parallelepiped one whose one sidelength, L_1 , was twice of the length of the other two sides, L_2 and L_3 . The explicit values were $L_1 = 2.222 \text{ nm}$ and $L_2 = L_3 = 1.111 \text{ nm}$. In the system 2, the Q_{\min} was 2.8 nm^{-1} ($=2\pi/L_1$). The FPMD simulation of the system 2 was carried out during 75 ps, which corresponds to 25 000 steps.

The structure factor, $S(Q)$, and the radial distribution function, $g(r)$, were evaluated by the conventional methods.⁸³ The mean square displacement of atoms (MSD), $\langle [\mathbf{r}(t) - \mathbf{r}(0)]^2 \rangle$ [$\mathbf{r}(t)$: position vector of atom at time t ; $\langle \cdot \cdot \rangle$: thermal average], was calculated in a conventional manner by averaging over all atoms and time origins in the whole MD steps. The velocity autocorrelation function (VAF), $\langle \mathbf{v}(t) \cdot \mathbf{v}(0) \rangle$ [$\mathbf{v}(t)$: velocity vector of atom at time t], was calculated similarly. The spectral density of the VAF, $\tilde{Z}(\omega)$, was calculated by the Fourier transform of the VAF. The self-diffusion coefficient, D , was obtained from both the

MSD and the time integral of the $Z(t)$ based on the well known equations^{32,84}

$$D = \lim_{t \rightarrow \infty} \frac{\langle [\mathbf{r}(t) - \mathbf{r}(0)]^2 \rangle}{6t} = \lim_{t \rightarrow \infty} \frac{\text{MSD}}{6t}, \quad (1)$$

$$D = \frac{1}{3} \int_0^\infty Z(t) dt. \quad (2)$$

The dynamic structure factor, $S(Q, \omega)$, was calculated in terms of the intermediate scattering function, $F(Q, t)$, which is defined as the space Fourier transform of the van Hove correlation function, $G(r, t)$:³²

$$F(Q, t) = \int d^3\mathbf{r} \exp(-i\mathbf{Q} \cdot \mathbf{r}) G(r, t) \quad (3)$$

$$= \frac{1}{N} \langle n_{\mathbf{Q}}(t) n_{-\mathbf{Q}}(0) \rangle. \quad (4)$$

In this equation, N is the number of atoms; the notation, $n_{\mathbf{Q}}(t)$, is the Fourier transform of the number density operator and defined explicitly as

$$n_{\mathbf{Q}}(t) = \sum_{j=1}^N \exp\{-i\mathbf{Q} \cdot \mathbf{r}_j(t)\}. \quad (5)$$

The $S(Q, \omega)$ is given as

$$S(Q, \omega) = \frac{1}{2\pi} \int dt \exp(-i\omega t) F(Q, t). \quad (6)$$

That is, the $S(Q, \omega)$ corresponds to the spectral density of the $F(Q, t)$ at a given wave number, Q .

III. RESULTS AND DISCUSSIONS

The present FPMD simulation is characterized by a long simulation time, the realization of a low Q value, and the investigation of the system size dependence. For the system 2 in the present FPMD simulation, the simulation time was taken to be 75 ps. The long simulation time and the low Q value, realized by the rectangular parallelepiped cell, are very effective to calculate the dynamic properties of liquids, particularly the dynamic structure factor and the dispersion relation for the longitudinal vibrational mode.

A. Static properties-structure factor, radial distribution function, bond angle distribution function, and coordination number distribution

The obtained $S(Q)$'s of the systems 1 and 2 for liquid Ge at 1253 K were compared with the typical experimental ones,^{1,3,5} as shown in Fig. 1. The first peak position of the $S(Q)$ in the present FPMD simulation was in good agreement with previous experiments.^{1,3,5} The shoulder of the experimental $S(Q)$ (Refs. 1–5) was also reasonably well reproduced by the present FPMD simulation irrespective of the boundary condition (system 1 or system 2).

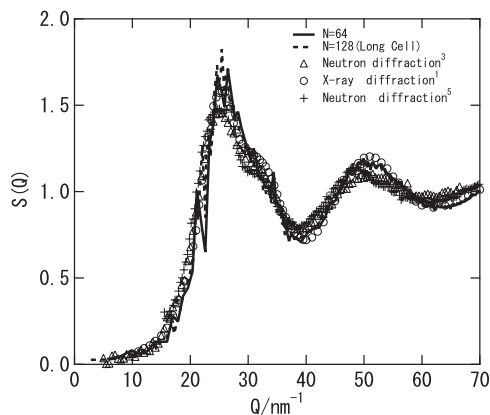


FIG. 1. Static structure factor, $S(Q)$, of liquid Ge at 1253 K. The solid line represents the $S(Q)$ obtained by the present FPMD (first-principles molecular-dynamics) simulation of 64 atoms (cubic cell: system 1) and the dotted line is that of 128 atoms [long cell (rectangular parallelepiped cell): system 2]. The open circle indicates the $S(Q)$ obtained by the x-ray diffraction (Ref. 1); the open triangle and the cross are the experimental $S(Q)$'s by the neutron diffraction in Refs. 3 and 5, respectively.

In Fig. 2 was shown the obtained $g(r)$'s of the systems 1 and 2 for liquid Ge at 1253 K, together with the experimental ones.^{1,3} The first peak for the system 2 is only a little lower and broader than that for the system 1. The position and the height of the first peak of the $g(r)$, particularly for the system 1 in the present FPMD simulation, were in good agreement with those obtained by the x-ray diffraction experiment by Waseda.¹ The characteristic feature of the $g(r)$ for liquid Ge is the enhanced tendency between the first peak distance and the second one. In this r range the small hump was reported in the previous experiments¹⁻⁴ instead of the minimum, which is observed for simple liquid metals, such as liquid alkali metals. This enhanced tendency was repro-

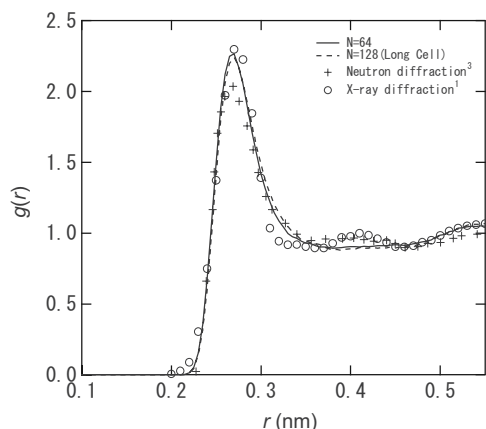


FIG. 2. Radial distribution function, $g(r)$, of liquid Ge at 1253 K. The solid line represents the $g(r)$ obtained by the present FPMD (first-principles molecular-dynamics) simulation of 64 atoms (cubic cell: system 1) and the dotted line is that of 128 atoms [long cell (rectangular parallelepiped cell): system 2]. The open circle and the cross indicate the $g(r)$'s obtained by the x-ray diffraction (Ref. 1) and by the neutron diffraction (Ref. 3), respectively.

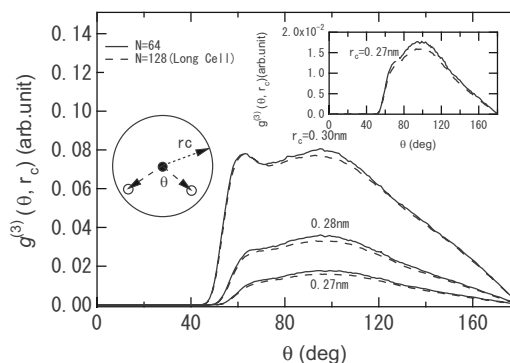


FIG. 3. Bond-angle distribution function, $g^{(3)}(\theta, r_c)$ of liquid Ge at 1253 K. The solid line represents the $g^{(3)}(\theta, r_c)$ obtained by the present FPMD (first-principle molecular-dynamics) simulation of 64 atoms (cubic cell: system 1) and the dotted line is that of 128 atoms [long cell (rectangular parallelepiped cell): system 2]. The inset is the magnified $g^{(3)}(\theta, r_c)$ for $r_c=0.27$ nm [the first peak distance of the $g(r)$].

duced by a rather flat shape in the present FPMD simulation, as can be seen in Fig. 2.

The calculated bond-angle distribution function, $g^{(3)}(\theta, r_c)$, was presented in Fig. 3. The bond angle, θ , was defined by a pair of vectors drawn from a reference atom to any other two atoms within the sphere of the cutoff radius, r_c . When the r_c is 0.3 nm, which is longer than the first peak distance of the $g(r)$, 0.27 nm, the $g^{(3)}(\theta, r_c)$ shows a clear peak centered around 60° in addition to a broad peak around 100° . When an interionic interaction is isotropic and, as is the case of simple liquids, the atoms are closely packed, the $g^{(3)}(\theta, r_c)$ should have a peak around 60° . Therefore, the peak around 60° in the present FPMD simulation indicates the existence of the typical structure of simple liquids in liquid Ge. Another peak angle, 100° , is close to the tetrahedral bond angle of 109° . With decreasing the r_c , the peak around 60° disappears. As can be clearly shown in the inset of Fig. 3, the $g^{(3)}(\theta, r_c)$ for $r_c=0.27$ nm shows only a single broad peak near 100° . This peak suggests that some local structure derived from anisotropic interactions remains in liquid Ge. Similar tendency of the $g^{(3)}(\theta, r_c)$ was already reported in the previous FPMD simulations⁵⁶⁻⁵⁹ with a boundary condition of a cubic box. The peak around 100° for the system 2 is only slightly lower than that for the system 1. Anyway, both results indicate that at least the fragment of tetrahedral structure unit seems to be present in liquid Ge.

The coordination number distribution was shown in Fig. 4. The coordination number of nearest neighbor atoms is usually evaluated from the $g(r)$.¹ However, the conventional method¹ for this evaluation is not easy for the case of liquid Ge, whose $g(r)$ has no first minimum, as shown in Fig. 2. Therefore, the coordination number, N , was evaluated as a number of atoms within the sphere of the cutoff radius, r_c , around a certain Ge atom. The $d(N)$ is defined as the frequency of the appearance of N . In the present FPMD simulation, the coordination number distribution, $d(N)$ - N relation, was given somewhat in detail for various r_c 's compared with the previous FPMD ones^{56,58,62} of cubic boundary condition. The slight dependence of the $d(N)$ on the boundary condition

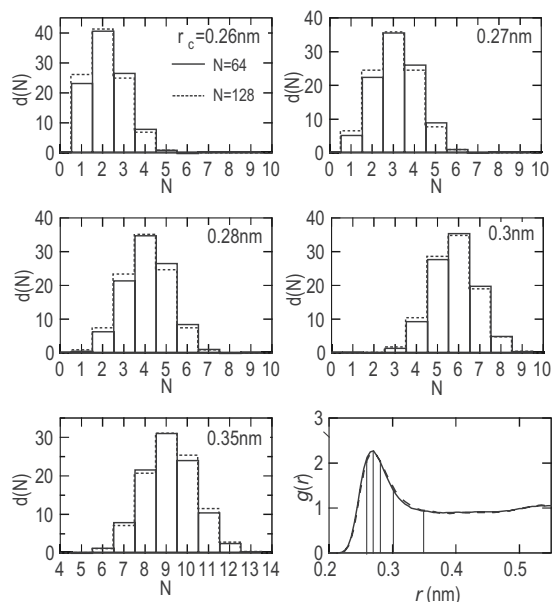


FIG. 4. Change of the coordination number distribution at 1253 K with the variation of cutoff radius, r_c [three figures in the left side and two figures (top and middle) in the right side]; N : Coordination number; $d(N)$: frequency of appearance of N . The box written by the solid line and that by the dotted line show the $d(N)$ for the system of 64 atoms (cubic cell: system 1) and that of 128 atoms [long cell (rectangular parallelepiped cell): system 2], respectively. The bottom figure in the right side shows the radial distribution function of liquid Ge [solid line: cubic cell (system 1); dashed line: rectangular parallelepiped cell (system 2)], in which the cutoff radii, r_c 's, for the evaluation of the $d(N)$'s were indicated by the vertical lines.

can be seen in Fig. 4; by changing the boundary condition from the system 1 to the system 2, the $d(N)$ for $r_c \leq 0.3$ nm shifts only slightly to the smaller N direction and the $d(N)$ for $r_c = 0.35$ nm shifts only slightly to the larger N direction. For the larger r_c 's (≥ 0.3 nm), the maximum coordination number, MCN, is 6–9, which is smaller than the coordination number of nearest neighbor atoms for simple liquid metals, 10–11.¹ This indicates that liquid Ge has a loose structure compared with simple liquid metals. On the other hand, the MCN shifts to smaller values, 2–4, with the decrease of the r_c . This may also show a possibility that in liquid Ge there exists a pair or a triplet of Ge atoms joined by the covalent bond.

In the present FPMD simulation, only a slight influence of the boundary condition was observed on $g(r)$, $g^{(3)}(\theta, r_c)$, and $d(N)$, as described above. The boundary condition of the system 1 may be slightly restrictive compared with that of the system 2, though obtained essential features are common to both systems.

B. Atomic dynamics-mean square displacement, self-diffusion coefficient, velocity autocorrelation function and its spectral density, and dynamic structure factor

The obtained MSD and relative VAF, given by $Z(t)/Z(0)$, were shown in Figs. 5 and 6, respectively. The solid and

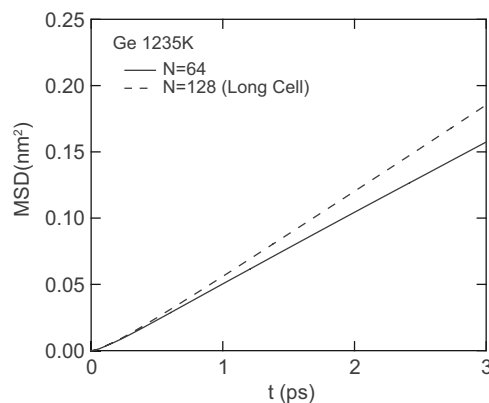


FIG. 5. Time variation of the mean square displacement (MSD), of atoms in liquid Ge at 1253 K. The solid and dashed lines show the MSD for the system of 64 atoms (cubic cell: system 1) and that of 128 atoms [long cell (rectangular parallelepiped cell): system 2], respectively.

dashed lines represent the results obtained by the systems 1 and 2, respectively. In Fig. 5 the MSD shows a free-particlelike behavior until about 0.1 ps and then follows a straight line (Brownian motion) in a long time region with an excellent statistical accuracy. As depicted in Fig. 6, the VAF shows almost only a positive region. This implies that the cage effect is almost absent in liquid Ge. One important feature of the structure of liquid Ge is a loose packing of atoms. As already discussed,²³ liquid Si and Ge are classified into the loosely packed liquid among the group 14 elements in the liquid state. The packing fractions just above the T_m of these liquids are only 0.30–0.33, which is far smaller than 0.45 for liquid Sn and Pb. This loose packing of atoms may be responsible for the almost absence of the cage effect in liquid Ge.

The D was evaluated from both the MSD and the time integral of the VAF. The D estimated from the MSD for $1 \text{ ps} < t < 3 \text{ ps}$ was found to be $0.89 \times 10^{-8} \text{ m}^2 \text{ s}^{-1}$ for the system 1 and $1.07 \times 10^{-8} \text{ m}^2 \text{ s}^{-1}$ for the system 2. The D from the time integral of the VAF is $0.92 \times 10^{-8} \text{ m}^2 \text{ s}^{-1}$ for

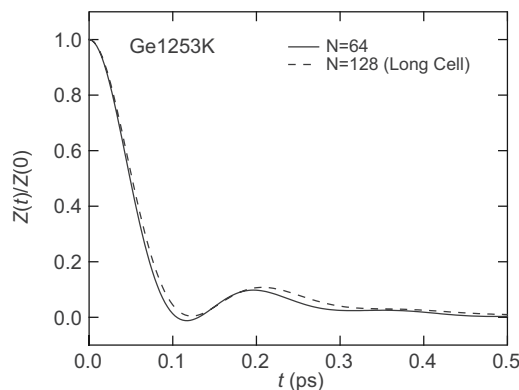


FIG. 6. Relative velocity autocorrelation function, $Z(t)/Z(0)$ [$Z(t)$: the velocity autocorrelation function at time t], for liquid Ge at 1253 K. The solid and dashed lines show the $Z(t)/Z(0)$ for the system of 64 atoms (cubic cell: system 1) and that of 128 atoms [long cell (rectangular parallelepiped cell): system 2], respectively.

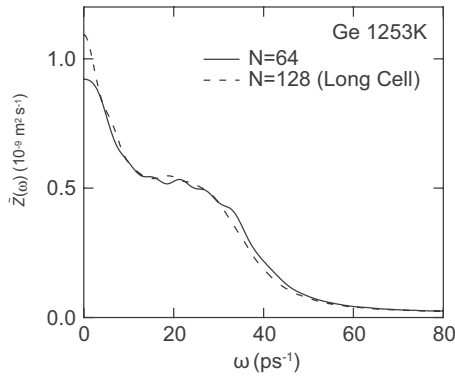


FIG. 7. Spectral density, $\tilde{Z}(\omega)$, of liquid Ge at 1253 K. The solid and dashed lines show the $\tilde{Z}(\omega)$ for the system of 64 atoms (cubic cell: system 1) and that of 128 atoms [long cell (rectangular parallelepiped cell): system 2], respectively.

the system 1 and $1.09 \times 10^{-8} \text{ m}^2 \text{ s}^{-1}$ for the system 2. The D of the system 2 is about 20% larger than that of the system 1. The comparatively restrictive boundary condition of the system 1 may give the smaller D compared with the system 2. This means that, in a small scale simulation like the present FPMD simulation, the periodic boundary condition and the number of atoms may affect the dynamic properties of liquids far remarkably compared with the static properties of liquids.

The spectral density, $\tilde{Z}(\omega)$, of the VAF was represented in Fig. 7. A subsidiary peak or bump is superimposed around 30 ps^{-1} on the main spectrum of the Brownian (diffusional) motion.⁸⁵ This subsidiary peak may support the existence of the propagating longitudinal vibrational mode in liquid Ge, which is a collective dynamics of atoms and is clearly shown by the side peaks in the $S(Q, \omega)$ described later. A similar subsidiary peak of the $\tilde{Z}(\omega)$ was also reported in the previous FPMD simulations.^{56,58} Kresse and Hafner⁵⁶ stressed that the bump around 30 ps^{-1} is related to the existence of the propagating longitudinal vibrational mode. As an evidence for this relation, they showed that a peak around 30 ps^{-1} of the vibrational density of states, $n_\nu(E)$, for the amorphous Ge, which was obtained by the FPMD simulation, corresponds to the experimental longitudinal acoustical peak in the $n_\nu(E)$ of polycrystalline Ge.

In Figs. 8 and 9, obtained $S(Q, \omega)$'s for $2.0 \text{ nm}^{-1} < Q < 12 \text{ nm}^{-1}$ and $17 \text{ nm}^{-1} < Q < 28 \text{ nm}^{-1}$ are shown, respectively, together with the experimental ones.³⁴ As can be seen in these figures, the present FPMD simulations for both the systems 1 and 2 well reproduce two characteristic features of the experimental $S(Q, \omega)$,³⁴ the presence of side peaks around the main peak in the low Q region below 12 nm^{-1} (Fig. 8) and the “de Gennes narrowing” of the main peak around $Q=24 \text{ nm}^{-1}$ (Fig. 9), which is very close to the Q_P (25.6 nm^{-1}) of the $S(Q)$ ¹⁻⁵ for liquid Ge (Fig. 1). The former feature is derived from the propagating longitudinal vibrational mode.³¹⁻³³ In the present FPMD study the presence of such longitudinal collective mode in liquid Ge was confirmed from both the $S(Q, \omega)$ and the $\tilde{Z}(\omega)$. The latter feature, the “de Gennes narrowing,” indicates the existence of

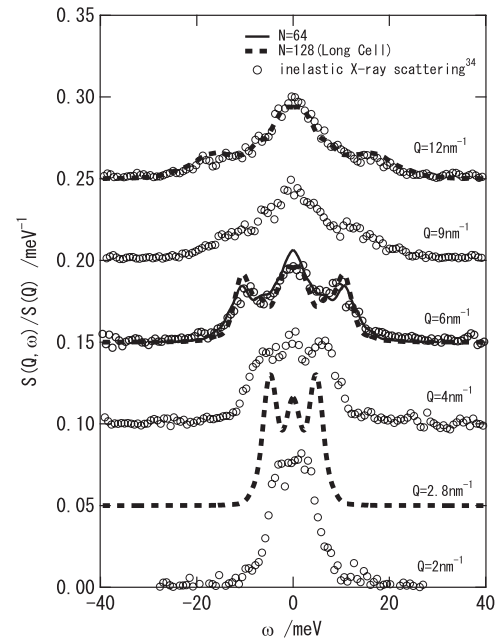


FIG. 8. Dynamic structure factor, $S(Q, \omega)$, divided by the static structure factor, $S(Q)$, $S(Q, \omega)/S(Q)$, of liquid Ge for $2.0 \text{ nm}^{-1} < Q < 12 \text{ nm}^{-1}$ at 1253 K. The solid line shows the $S(Q, \omega)/S(Q)$ obtained for the system of 64 atoms (cubic cell: system 1). The dotted line represents that of 128 atoms [long cell (rectangular parallelepiped cell): system 2]. The open circles show the experimental values (Ref. 34).

the component of density fluctuation with a long decay time corresponding to the Q_p ,^{32,33} at which the $S(Q)$ has the large peak value. This long decay time can be understood from the presence of the $S(Q)$ in the denominator of the theoretical expression^{32,33,86} for the width of the main peak in the $S(Q, \omega)$. Physically speaking, the Q component of the density-density correlation, which can be originally represented by the $S(Q)$, is largest at Q_p . Therefore, around Q_p , the $F(Q, t)$, which corresponds to the density autocorrelation function, decays considerably slowly.³² As a result, the narrowing occurs for the $S(Q, \omega)$, which is the spectral density of the $F(Q, t)$. Hosokawa *et al.*³⁶ reported that the “de Gennes narrowing” in liquid Si is observed at substantially lower Q (20 nm^{-1}) than the Q_p (27 nm^{-1}). As for this problem, further studies must be performed experimentally and theoretically.

C. Atomic dynamics-dispersion relation

In Fig. 10 the dispersion relation, ω_p - Q relation, in the present FPMD simulation was compared with that given by the IXS experiment by Hosokawa *et al.*³⁴ The good agreement of the dispersion relation for liquid Ge was obtained between the present FPMD simulation and the IXS experiment.³⁴ It is worth mentioning that for the first time the present FPMD simulation realized the comparison between the simulated dispersion relation and the IXS experiment³⁴ by adopting a small Q value obtained by the rectangular parallelepiped cell (system 2), though it is a fact that Mune-

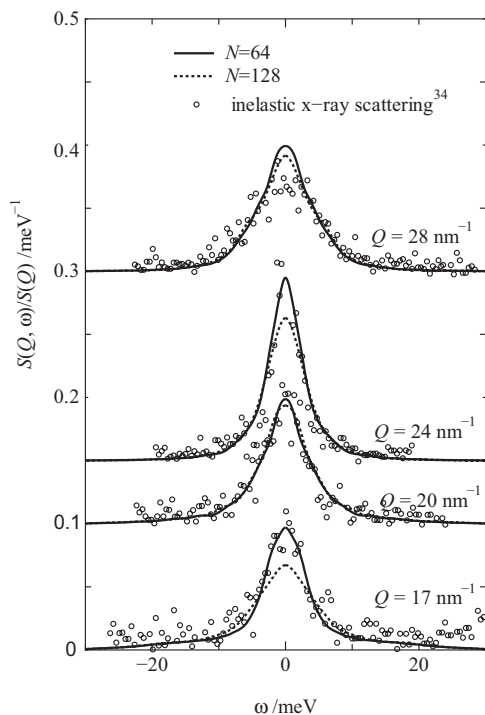


FIG. 9. Dynamic structure factor, $S(Q, \omega)$, divided by the static structure factor, $S(Q)$, $S(Q, \omega)/S(Q)$, of liquid Ge for $17 \text{ nm}^{-1} < Q < 28 \text{ nm}^{-1}$ at 1253 K. The solid line shows the $S(Q, \omega)/S(Q)$ obtained for the system of 64 atoms (cubic cell: system 1). The dotted line represents that of 128 atoms [long cell (rectangular parallelepiped cell): system 2]. The open circles show the experimental values (Ref. 34).

jiri *et al.*⁶⁰ and Chai *et al.*⁶¹ have already presented some comments about such a comparison. Hugouviex *et al.*⁶² showed that the ω_p 's obtained by their FPMD simulation in the high Q ($\geq 7 \text{ nm}^{-1}$) region are well situated on the experimental dispersion relation of Hosokawa *et al.*,³⁴ though there exists a difference between the temperature of their simulation and that of the IXS experiment by Hosokawa *et al.*³⁴ As shown in Fig. 10, with the increase of the Q , the ω_p in the present FPMD simulation increases with the gradient which is very close to the experimental velocity of sound, 2682 ms^{-1} .³⁸ That is, the present FPMD simulation well reproduced the “no positive dispersion” for liquid Ge.³⁴ In Fig. 10 the ω_p seems to show a slight depression tendency in the Q range over 8 nm^{-1} . This suppression tendency may be derived from the “structure effect,”^{37,63} as already described.

As described in the Introduction, it is not easy to understand the “no positive dispersion” for liquid Ge from the existing view points. Particularly we stress that the MC theory may be invalid for the explanation of “positive dispersion” of liquids. The main reason for it is the breakdown of the MC theory for liquid Na at 900 K (Ref. 75) in spite of the existence of “positive dispersion” up to 1173 K.⁷⁶ Casas *et al.*⁷² showed a fair success in the explanation of the physical properties of atomic dynamics for liquid Li up to a considerably high temperature, 843 K, based on the self-consistent treatment of the MC theory,⁸⁷ in which the input structure information was calculated by the variational modi-

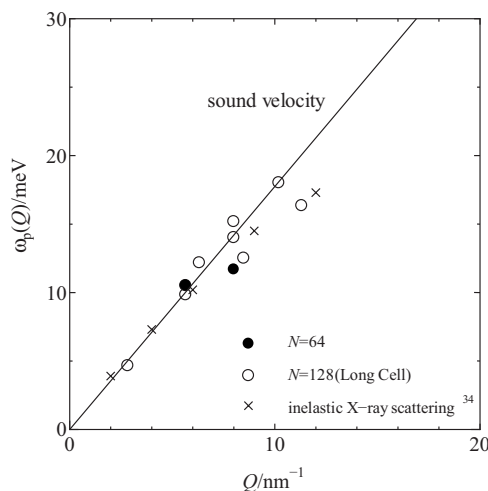


FIG. 10. Dispersion relation, ω_p-Q , of liquid Ge [ω_p : the peak angular frequency of the side peaks in the $S(Q, \omega)$ at the wave number Q]. The solid and open circles show the data of the system of 64 atoms (cubic cell: system 1) and those of 128 atoms [long cell (rectangular parallelepiped cell): system 2], respectively. The cross shows the experimental data (Ref. 34). The solid line (“sound velocity”) is the dispersion relation drawn by the experimental sound velocity in liquid Ge (Ref. 38).

fied hypernetted chain approximation.⁸⁸ Unfortunately, the interionic pair potential, which has a key role for the validity of the MC theory, was not shown in this paper. However, if the normalized temperature by the T_m is adopted, liquid Li at 843 K ($1.86 T_m$) is closer to the T_m , compared with liquid Na at 900 K ($2.43 T_m$). In addition, even at 843 K ($1.86 T_m$) the VAF keeps clear cage effect (negative region)⁸⁹ compared with the case of liquid Na at high temperatures.⁷⁵ Moreover, liquid Li at 843 K is far viscous than liquid Na at 900 K judging from their viscosity values,⁹⁰ the shear viscosity and the kinematic viscosity of liquid Li at 843 K are 29.918 Pa s and $6.25 \times 10^{-7} \text{ m}^2 \text{ s}^{-1}$, respectively and those of liquid Na at 900 K are 20.057 Pa s and $2.50 \times 10^{-7} \text{ m}^2 \text{ s}^{-1}$, respectively. Thus, in spite of its validity for liquid Li at 843 K, the MC theory seems to be surely invalid for liquid Na at 900 K and accordingly other methods must be considered for the explanation of the dispersion relation in liquids. Therefore, we simply present very primitive discussions about the problem “no positive dispersion” for liquid Ge.

As for liquid Ge, we can list particular features, loosely packed structure, rather soft (“ledge-type” or “nonharsh”) interionic pair potential, and low kinematic viscosity, $\nu(\text{m}^2 \text{ s}^{-1})$. The ν is defined as η/ρ in which $\eta(\text{Kg m}^{-1} \text{ s}^{-1})$ is the shear viscosity and $\rho(\text{Kg m}^{-3})$ is the density; in the parenthesis the dimension is written. The first point, the loosely packed structure or the small packing fraction, seems to make the application of the MC theory difficult, because of the suppression for the slow decay relaxation mechanism in the MC theory.⁷⁵ In addition, this makes the proposed factor F , described below, small. However, apart from such intuitive views, at least for liquid metals, the decrease of the packing fraction with the increase of the temperature enlarges the softness of the interionic pair potential, as shown

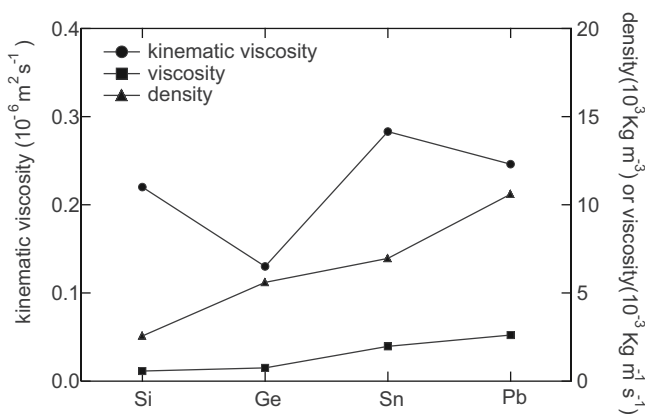


FIG. 11. Density, viscosity (shear viscosity), and kinematic viscosity of the group 14 elements in the liquid state. The data sources for the density and viscosity (shear viscosity) should be referred to the text.

by Hoshino *et al.*⁷⁵ for liquid Na because of its density dependence. Therefore, the problem of low packing for liquid metals seems to reduce to that of interionic pair potential, the second point. The second point, the soft or moderately repulsive interionic pair potential at the nearest neighbor distance (“ledge-type” or “nonharsh” feature) for liquid Ge (Refs. 7, 8, 14, 17, 50, and 75) also makes the “positive dispersion” weaker, as discussed by Balucani and Zoppi.³³ Quite recently we found the third point, the low kinematic viscosity of liquid Ge. Accurate experimental values of the shear viscosity are available for liquid Si,^{29,30} Ge,²⁹ Sn,⁸⁴ and Pb.⁸⁴ The density data are also available for these liquid metals.^{29,91,92} By using these data the ν can be calculated for the group 14 elements in the liquid state. As shown in Fig. 11, the ν of liquid Ge ($1.3 \times 10^{-7} \text{ m}^2 \text{ s}^{-1}$) with “no positive dispersion”³⁴ is very low (only half) compared with that of liquid Si and Sn with “positive dispersion,”^{36,93} It is also lower than that of liquid Pb, for which, up to date, no dispersion relation has been reported. It should be noted that liquid Na at 1173 K, which shows a “positive dispersion”^{37,76} in spite of high temperature, still keeps a high value of the ν , $2.12 \times 10^{-7} \text{ m}^2 \text{ s}^{-1}$.⁹⁰ Liquid Ge near the T_m is less viscous than liquid Na at 1173 K.

We propose the parameter, F , defined by $(\nu/a)y$ [a : first peak distance of the $g(r)$; y : packing fraction]. This parameter was defined so that the dimension of F may be same as that of the velocity of sound. The values of a and y were taken from Waseda¹ and Itami *et al.*,²³ respectively. In addition, we can calculate the positive dispersion (%), PDP , for these liquid metals from the Table I in the elaborate review by Scopigno *et al.*³⁷ The data set, (F, PDP) , for liquid Si, Ge, and Sn are respectively (0.27, 16), (0.16, 0), and (0.36, 12). We note that the “no positive dispersion” appears only in the case of small F , which is derived from the small packing fraction and the low kinematic viscosity. Judging from the similar values of the packing fraction, y , between liquid Ge and liquid Si, the kinematic viscosity may be most responsible for the “no positive dispersion” of liquid Ge. By now, the role of the kinematic viscosity has been discussed implicitly in the theories of the transverse wave in liquids.^{31–33} It is

a future theoretical problem to clarify the effect of the kinematic viscosity on the propagating longitudinal vibrational mode in liquids. Anyway the “no positive dispersion” for liquid Ge may be related to the particular features of liquid Ge, loosely packed structure, soft (“ledge-type” or “nonharsh”) interionic pair potential, and low kinematic viscosity. The collective atomic dynamics and the “no positive dispersion” for liquid Ge should be studied further more experimentally and theoretically.

D. Atomic dynamics-trace and environment analysis of the single atomic motion

From the analysis of the experimental $S(Q, \omega)$ for liquid Si, Hosokawa *et al.*³⁶ showed the existence of the fast (sub-picosecond) mode, which corresponds to a short time correlation between neighboring atoms derived from the covalent bonds in liquid Si shown by the FPMD simulation by Štich *et al.*⁹⁴ The importance of fast and slow modes has been recently stressed for liquid Li.^{37,63} It is also important to investigate whether such dynamical modes are present in liquid Ge or not. Thus, there exists a complicated problem for the understanding of the atomic dynamics in liquid Ge. To establish the microscopic theory of atomic dynamics in liquid Ge, the detailed analysis must be performed for the characteristic feature of atomic motion in liquid Ge.

The detailed investigation was performed in the present FPMD simulation to clarify the trace and environment of the single atomic motion in liquid Ge. As shown in Fig. 12, the analyzed quantities were the time variation of the tag number of surrounding atoms around atom 1 within the sphere with a cutoff radius of 0.27 nm, which corresponds to the first peak distance of the $g(r)$ (a), the scalar product, $v_1(t) \cdot v_{1c}(t)$, between the velocity vector of atom 1 and the average velocity vector of coordinated atoms around atom 1 (b), the x , y , and z components (F_1^x , F_1^y , and F_1^z) of the force acting on atom 1, F_1 (c), the coordination number, N_1 , calculated as the number of atoms around atom 1 within the sphere with a cutoff radius of 0.27 nm (d), the MSD and the square displacement of atom 1 (e). Figure 12(c) indicates that atom 1 moves under the fluctuating random force, as expected from the Langevin equation. As can be seen in Fig. 12, there exist five characteristic periods, 0.1–0.4 ps (period I), 0.4–0.6 ps (period II), 0.7–1.2 ps (period III), 1.2–1.7 ps (period IV), and 1.7–2.0 ps (period V).

In period I, because of the small N_1 (0–2), atom 1 moves largely in the inverse direction to the coordinated atoms [(b) $v_1(t) \cdot v_{1c}(t) < 0$, (d), and (e)]. In this period, there even exists a time at which no coordinated atoms are present around atom 1(a). In the period II, atom 1 advances rather moderately with the increase of the N_1 (1–3) [(d) and (e)]. In the period III, with the further increase of the N_1 (1–4), atom 1 moves rather backwardly together with coordinated atoms [(b) $v_1(t) \cdot v_{1c}(t) > 0$, (d), and (e)]. There exists a considerably long time at which atom 1 is surrounded by same 3 or 4 coordinated atoms (a). In addition, the $v_1(t) \cdot v_{1c}(t)$ keeps a distinct positive value. These imply the existence of the movement as an atomic group joined by the covalent bond. In fact, the snap shot of the electron density profile in the

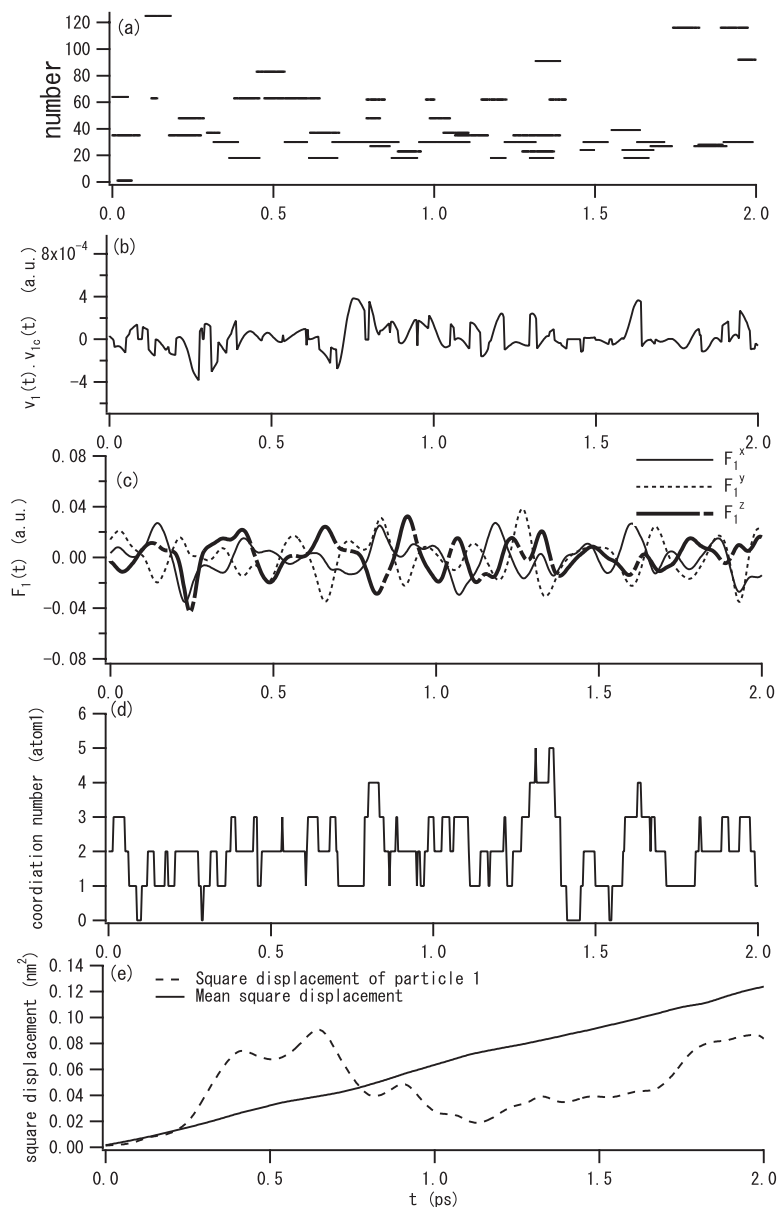


FIG. 12. Trace and environment analysis of the single atomic motion in liquid Ge by the FPMD simulation of 128 atoms [long cell (rectangular parallelepiped cell): system 2]; (a) the time variation of the number (tag number) of atoms which are present within the sphere with a cutoff radius of 0.27 nm [the first peak distance of the radial distribution, $g(r)$] around atom 1; (b) that of the $v_1(t) \cdot v_{1c}(t)$, the scalar product between the velocity vector of atom 1 and the average velocity vector of coordinated atoms around atom 1; (c) that of the x , y , and z components (F_1^x , F_1^y , and F_1^z) of the force acting on atom 1, F_1 ; (d) that of the coordination number (N_1) calculated as the number of surrounding atoms around atom 1 within the sphere with a cutoff radius of 0.27 nm; (e) the comparison between the time variation of the mean square displacement (MSD) and the square displacement of atom 1.

present FPMD simulation shows the increase of the electron density between Ge atoms compared with the case of the superposition of free atoms, as found for liquid Ge by Takeuchi and Garzón⁵⁸ and for liquid Si by Štich *et al.*⁹³ A moderate advance of atom 1 with slightly positive $v_1(t) \cdot v_{1c}(t)$ in the period II may be derived also from a atomic group motion containing 2–4 atoms. In the period IV, atom 1 does not move significantly because of the large N_1 (1–5) [(d) and (e)]. Also in this period, the same 3 or 4 coordinated atoms sometimes stay around atom 1 during considerably a long time (a). Moreover, the $v_1(t) \cdot v_{1c}(t)$ is fluctuating around zero (b). These imply the trapping of atom 1 in a cage of neighboring atoms. The cage effect seems to be present microscopically, though it is almost absent from the VAF. Clearer microscopic cage effect, seen in this period IV in the present FPMD study, was observed for the system 1 in the previous FPMD simulation.⁶⁰ In the period V, the forward movement of atom 1 occurs moderately under the restriction of slightly

large N_1 (1–3) [(d) and (e)]. The decoupling into the periods I–V in the present study contains somewhat an ambiguity. Moreover, the features described above are slightly dependent on the window we observe. Nevertheless, we can summarize the analysis for the trace and environment of single atomic motion, as follows: The single atomic motion proceeds in the case of the small N_1 (0–2) and is restrained in the case of the large N_1 (3–4); the latter is derived from the microscopic cage effect and the suppression of the atomic migration by the formation of the atomic group of 3–5 atoms, which implies the existence of covalent bond even in the liquid state of Ge.

IV. SUMMARY

The static and dynamic properties of liquid Ge were investigated in detail by the FPMD simulation with a long simulation time and a large cell. The present FPMD simula-

tion well reproduces the experimental static structure factors. In addition, it reproduces well the characteristic features of the dynamic structure factors, the existence of the side peaks and the “de Gennes narrowing.” It was shown that the self-diffusion coefficient for the system 2 (rectangular parallel-piped cell) of 128 atoms is about 20% larger than that for the system 1 (cubic cell) of 64 atoms. The “no positive dispersion” for liquid Ge, which was found by Hosokawa *et al.*,³⁴ was also well reproduced. The reason for this “no positive dispersion” was discussed with particular attention to the low kinematic viscosity of liquid Ge. The detailed trace and environment analysis of the atomic motion seems to indicate the suppression of single atomic motion by the microscopic

cage effect and the formation of the atomic group joined by the covalent bond.

ACKNOWLEDGMENTS

We are grateful to S. Hosokawa and Y. Kawakita for providing us with their experimental data. This study was performed in the definition phase activity of the selected subject as the candidate for the International Announcement of Opportunity (IAO) for the microgravity experiment on the International Space Station (ISS). We are grateful also to many organizations and scientists relevant to IAO and ISS for providing us with the opportunity to perform the present study.

*Present address: Graduate School of Integrated Arts and Sciences, Hiroshima University, Higashi-Hiroshima, 739-8521, Japan.
 †Present address: Institute of Technology, Shibaura Institute of Technology 3-7-5 Toyosu, Koto-ku, Tokyo 135-1548 Japan.
 ‡Corresponding author. itami@sci.hokudai.ac.jp, FAX.: +81-11-706-4841.
¹Y. Waseda, *The Structure of Non-Crystalline Materials, Liquid and Amorphous Solid* (McGraw-Hill, New York, 1980).
²P. S. Salmon, *J. Phys. F: Met. Phys.* **18**, 2345 (1988).
³M. C. Bellisent-Funnel and R. Bellisent, *J. Non-Cryst. Solids* **65**, 383 (1984).
⁴Th. Altenholz and W. Hoyer, *J. Non-Cryst. Solids* **250-252**, 48 (1999).
⁵Y. Kawakita, S. Takeda, T. Enosaki, K. Oshima, H. Aoki, T. Masaki, and T. Itami, *J. Phys. Soc. Jpn.* **71**, 12 (2002).
⁶T. Itami, S. Munejiri, T. Masaki, H. Aoki, Y. Ishii, T. Kamiyama, Y. Senda, F. Shimojo, and K. Hoshino, *Phys. Rev. B* **67**, 064201 (2003).
⁷J. Hafner and G. Kahl, *J. Phys. F: Met. Phys.* **14**, 2259 (1984).
⁸W. Jank and J. Hafner, *Phys. Rev. B* **41**, 1497 (1990).
⁹A. Harada, F. Shimojo, and K. Hoshino, *J. Phys. Soc. Jpn.* **74**, 2017 (2005).
¹⁰B. R. Orton, *Z. Naturforsch. A* **30**, 1500 (1975); **31**, 397 (1976); **32**, 332 (1977); **34**, 1547 (1979); B. R. Orton, *J. Phys. (Paris)* **41**, C8 (1980).
¹¹P. Gabather and S. Steeb, *Z. Naturforsch. A* **34**, 1314 (1979).
¹²V. Petkov and G. Yunchov, *J. Phys.: Condens. Matter* **6**, 10 885 (1994).
¹³M. Silbert and W. H. Young, *Phys. Lett.* **58A**, 469 (1976).
¹⁴M. J. Grimson and M. Silbert, *J. Phys. F: Met. Phys.* **14**, L95 (1984).
¹⁵I. Yokoyama and S. Ono, *J. Phys. F: Met. Phys.* **15**, 1215 (1985).
¹⁶K. Hoshino, C. H. Leung, L. McLaughlin, S. R. M. Rahman, and W. H. Young, *J. Phys. F: Met. Phys.* **17**, 787 (1987).
¹⁷G. Kahl and J. Hafner, *Solid State Commun.* **49**, 1125 (1984).
¹⁸Ya. Chushak, J. Hafner, and G. Kahl, *Phys. Chem. Liq.* **29**, 159 (1984).
¹⁹K. K. Mon, N. W. Ashcroft, and G. V. Chester, *Phys. Rev. B* **19**, 5103 (1979).
²⁰L. E. González, D. J. González, and G. Silbert, *Mol. Phys.* **99**, 875 (2001).
²¹N. W. Ashcroft, *Nuovo Cimento D* **12**, 597 (1990).

²²J. Hafner and V. Heine, *J. Phys. F: Met. Phys.* **13**, 2475 (1983).
²³T. Itami, T. Masaki, H. Aoki, S. Munejiri, M. Uchida, S. Matsumoto, K. Kamiyama, and K. Hoshino, *J. Non-Cryst. Solids* **312-314**, 177 (2002).
²⁴V. M. Glazov, S. N. Chizhevskaya, and N. N. Glagoleva, *Liquid Semiconductors* (Plenum, New York, 1969).
²⁵M. Cutler, *Liquid Semiconductors* (Academic Press, New York-San Francisco-London, 1977).
²⁶P. Pavlov and E. V. Dobrokhotov, *Sov. Phys. Solid State* **12**, 225 (1970).
²⁷T. Itami, H. Aoki, N. Higashimoto, T. Onogi, M. Kaneko, Y. Abe, Y. Arai, A. Tanji, M. Uchida, K. Iribe, H. Ando, K. Goto, N. Tateiwa, M. Koyama, T. Morita, H. Kawasaki, S. Yoda, N. Koshikawa, T. Masaki, H. Oda, T. Suzuki, T. Nakamura, and Y. Nakamura, *J. Jpn. Soc. Microgravity Appl.* **14**, 323 (1997); T. Itami, H. Aoki, N. Higashimoto, T. Onogi, K. Sugimura, M. Kaneko, Y. Abe, A. Tanji, M. Uchida, K. Iribe, H. Ando, K. Goto, N. Tateiwa, M. Koyama, T. Morita, H. Kawasaki, S. Yoda, N. Koshikawa, T. Masaki, H. Oda, T. Suzuki, T. Nakamura, and Y. Nakamura, *ibid.* **16**, 79 (1999).
²⁸S. Yoda, T. Masaki, and H. Oda, *J. Jpn. Soc. Microgravity Appl. Suppl. II* **15**, 343 (1998).
²⁹Y. Sato, T. Nishizuka, T. Tachikawa, M. Hoshi, T. Yamamura, and Y. Waseda, *High Temp. - High Press.* **32**, 239 (2000).
³⁰Y. Sato, Y. Kameda, T. Nagasawa, T. Sakamoto, S. Moriguchi, T. Yamamura, and Y. Waseda, *J. Cryst. Growth* **249**, 404 (2003).
³¹J. P. Boon and S. Yip, *Molecular Hydrodynamics* (Dover, New York, 1980).
³²J. P. Hansen and I. R. McDonald, *Theory of Simple Liquids*, 3rd ed. (Academic Press, UK-The Netherland-USA, 2006).
³³U. Balucani and M. Zoppi, *Dynamics of the Liquid State* (Oxford University Press, Oxford, 1994).
³⁴S. Hosokawa, Y. Kawakita, W.-C. Pilgrim, and H. Sinn, *Phys. Rev. B* **63**, 134205 (2001).
³⁵S. Hosokawa, Y. Kawakita, W.-C. Pilgrim, and H. Sinn, *Physica B* **316-317**, 610 (2002).
³⁶S. Hosokawa, W.-C. Pilgrim, Y. Kawakita, K. Oshima, S. Takeda, D. Ishikawa, S. Tsutsui, and A. Q. R. Baron, *J. Phys.: Condens. Matter* **15**, L623 (2003).
³⁷T. Scopigno, G. Ruocco, and F. Sette, *Rev. Mod. Phys.* **77**, 881 (2005).
³⁸N. Yoshimoto, H. Shibata, M. Yoshizawa, K. Suzuki, K. Shige-

- matsu, and S. Kimura, *Jpn. J. Appl. Phys., Part 1* **35**, 2754 (1996).
- ³⁹D. Ishikawa, M. Inui, K. Matsusita, K. Tamura, S. Tsutsui, and A. Q. R. Baron, *Phys. Rev. Lett.* **93**, 097801 (2004).
- ⁴⁰F. Demmel, S. Hosokawa, M. Lorenzen, and W.-C. Pilgrim, *Phys. Rev. B* **69**, 012203 (2004).
- ⁴¹U. Balucani, G. Ruocco, A. Torcini, and R. Vallaury, *Phys. Rev. E* **47**, 1677 (1993).
- ⁴²G. Monaco, A. Cunsolo, G. Ruocco, and F. Sette, *Phys. Rev. E* **60**, 5505 (1999).
- ⁴³S. C. Santucci, D. Fioretto, L. Comez, A. Gessini, and C. Masciovecchio, *Phys. Rev. Lett.* **97**, 225701 (2006).
- ⁴⁴T. Kamiyama, S. Hosokawa, A. Q. R. Baron, S. Tsutsui, K. Yoshida, W.-C. Pilgrim, Y. Kiyonagi, and T. Yamaguchi, *J. Phys. Soc. Jpn.* **73**, 1615 (2004).
- ⁴⁵T. Scopigno, E. Pontecorvo, R. Di Lenardo, M. Krish, G. Monaco, G. Ruocco, B. Ruzicka, and F. Sette, *J. Phys.: Condens. Matter* **15**, S1269 (2003).
- ⁴⁶T. Scopigno, R. Di Lenardo, G. Ruocco, A. Q. R. Baron, S. Tsutsui, F. Bossard, and S. N. Yannopoulos, *Phys. Rev. Lett.* **92**, 025503 (2004).
- ⁴⁷B. Ruzicka, T. Scopigno, S. Caponi, A. Fontana, Q. Pilla, P. Giura, G. Monaco, E. Pontecorvo, G. Ruocco, and F. Sette, *Phys. Rev. B* **69**, 100201(R) (2004).
- ⁴⁸L. E. Bove, F. Formisano, F. Sacchetti, C. Petrillo, A. Ivanov, B. Dorner, and F. Barocchi, *Phys. Rev. B* **71**, 014207 (2005).
- ⁴⁹F. J. Bermejo, R. Fernandez-Perea, M. Alvarez, B. Roessli, H. E. Fisher, and J. Bossy, *Phys. Rev. E* **56**, 3358 (1997).
- ⁵⁰K. Hoshino, *J. Phys. Soc. Jpn.* **71**, 2466 (2002).
- ⁵¹K. Hoshino, *Z. Phys. Chem.* **217**, 817 (2003).
- ⁵²A. Arnold, N. Mauser, and J. Hafner, *J. Phys.: Condens. Matter* **1**, 965 (1989).
- ⁵³W. Yu, Z. Q. Wang, and D. Stroud, *Phys. Rev. B* **54**, 13946 (1996).
- ⁵⁴N. W. Ashcroft and D. Stroud, *Solid State Physics* (Academic, New York, 1978), Vol. 33, p. 1.
- ⁵⁵F. H. Stillinger and T. A. Weber, *Phys. Rev. B* **31**, 5262 (1985).
- ⁵⁶G. Kresse and J. Hafner, *Phys. Rev. B* **49**, 14251 (1994).
- ⁵⁷G. Kresse and J. Hafner, *Phys. Rev. B* **47**, 558 (1993).
- ⁵⁸N. Takeuchi and I. L. Garzón, *Phys. Rev. B* **50**, 8342 (1994).
- ⁵⁹R. V. Kulkarni, W. G. Aulbur, and D. Stroud, *Phys. Rev. B* **55**, 6896 (1997).
- ⁶⁰S. Munejiri, F. Shimojo, K. Hoshino, and T. Itami, *J. Non-Cryst. Solids* **312-314**, 182 (2002).
- ⁶¹J.-Da Chai, D. Stroud, J. Hafner, and G. Kresse, *Phys. Rev. B* **67**, 104205 (2003).
- ⁶²V. Hugouvieux, E. Farhi, M. R. Johnson, F. Juranyi, P. Bourges, and W. Kob, *Phys. Rev. B* **75**, 104208 (2007).
- ⁶³T. Scopigno, U. Balucani, G. Ruocco, and F. Sette, *J. Phys.: Condens. Matter* **12**, 8009 (2000).
- ⁶⁴C. Cabrillo, F. J. Bermejo, M. Avalez, P. Verkerk, A. Maira-Vidal, S. M. Bennington, and D. Martin, *Phys. Rev. Lett.* **89**, 075508 (2002).
- ⁶⁵L. E. Bove, B. Dorner, C. Petrillo, F. Sacchetti, and J. Suck, *Phys. Rev. B* **68**, 024208 (2003).
- ⁶⁶D. Levesque, L. Verlet, and J. Kürkijarvi, *Phys. Rev. A* **7**, 1690 (1973).
- ⁶⁷Song-Ho Chong, *Phys. Rev. E* **74**, 031205 (2006).
- ⁶⁸W. Götze and M. R. Mayer, *Phys. Rev. E* **61**, 587 (2000).
- ⁶⁹U. Balucani, A. Torcini, and R. Vallaury, *Phys. Rev. B* **47**, 3011 (1993).
- ⁷⁰J. Casas, D. J. González, and L. E. González, *Phys. Rev. B* **60**, 10094 (1999).
- ⁷¹F. Shimojo, K. Hoshino, and M. Watabe, *J. Phys. Soc. Jpn.* **61**, 1821 (1994).
- ⁷²J. Casas, D. J. González, L. E. González, M. M. G. Alemany, and L. I. Gallego, *Phys. Rev. B* **62**, 12095 (2000).
- ⁷³L. E. González, D. J. González, and J. Casas, *J. Non-Cryst. Solids* **312-314**, 158 (2002).
- ⁷⁴W. Gudowski, M. Dzugutov, and M. Larsson, *Phys. Rev. E* **47**, 1693 (1993).
- ⁷⁵K. Hoshino, F. Shimojo, and S. Munejiri, *J. Phys. Soc. Jpn.* **71**, 119 (2002).
- ⁷⁶W.-C. Pilgrim, S. Hosokawa, H. Saggau, H. Sinn, and E. Burkel, *J. Non-Cryst. Solids* **250-252**, 96 (1999).
- ⁷⁷J. P. Perdew, K. Burke, and M. Ernzerhof, *Phys. Rev. Lett.* **77**, 3865 (1996).
- ⁷⁸M. P. Teter, M. C. Payne, and D. C. Allan, *Phys. Rev. B* **40**, 12255 (1989).
- ⁷⁹F. Shimojo, Y. Zempo, K. Hoshino, and M. Watabe, *Phys. Rev. B* **52**, 9320 (1995).
- ⁸⁰S. Nosé, *Mol. Phys.* **52**, 255 (1984).
- ⁸¹W. G. Hoover, *Phys. Rev. A* **31**, 1695 (1985).
- ⁸²H. Nakanishi, K. Nakazato, S. Asaba, K. Abe, S. Maeda, and K. Terashima, *J. Cryst. Growth* **191**, 711 (1998).
- ⁸³M. P. Allen and D. J. Tildersley, *Computer Imulation of Liquids* (Oxford University Press, Oxford-New York-Toronto, 1987); see also J. M. Haile, *Molecular Dynamics Simulation-Elementary Methods* (A Wiley-International Publications, New York-Chichester-Weinheim- Brisbane-Singapore-Toronto, 1992).
- ⁸⁴M. Shimojo and T. Itami, *Atomic Transport in Liquid Metals* (Trans. Tech. Pub., Switzerland, 1986).
- ⁸⁵P. A. Egelstaff, *An Introduction to the Liquid State* (Clarendon Press, Oxford, 1992).
- ⁸⁶E. G. D. Cohen, P. Westerhuijs, and I. M. de Schepper, *Phys. Rev. Lett.* **59**, 2872 (1987).
- ⁸⁷L. Sjögren and A. Sjölander, *J. Phys. C* **12**, 4369 (1979).
- ⁸⁸Y. Rosenfeld and N. W. Ashcroft, *Phys. Rev. A* **20**, 1208 (1979); T. Itami, in *Condensed Matter Disordered Solids*, edited by S. K. Srivastava and N. H. March (World Scientific, Singapore-New Jersey-London-Hong Kong, 1995), Chap. 3, p. 159.
- ⁸⁹M. Canales, L. E. González, and J. À. Padró, *Phys. Rev. E* **50**, 3656 (1994).
- ⁹⁰E. E. Shpil'rain, K. A. Yakimovich, V. A. Fomin, S. N. Skovorodjko, and A. G. Mozgovoï, in *Handbook of Thermodynamic Properties of Alkali Metals*, edited by R. W. Ohse (Blackwell Scientific Publications, Oxford-London-Edinburgh-Boston-Palo Alto-Melbourne, 1985), Chap. 7.3, p. 753.
- ⁹¹*Handbook of Chemistry and Physics*, 79th ed., edited By D. R. Lide (CRC Press, Boca Raton-Boston-London-New York-Washington, 1998).
- ⁹²Y. Sato, T. Nishizaki, K. Hara, T. Yamamura, and Y. Waseda, *Int. J. Thermophys.* **21**, 1463 (2000).
- ⁹³S. Hosokawa, J. Greif, F. Demmel, and W.-C. Pilgrim, *Chem. Phys.* **292**, 253 (2003).
- ⁹⁴I. Štich, R. Car, and M. Parrinello, *Phys. Rev. B* **44**, 4262 (1991).